SYBR Green-Based Real-Time Quantitative PCR Assay for Detection of West Nile Virus Circumvents False-Negative Results Due to Strain Variability

James F. Papin, Wolfgang Vahrson, and Dirk P. Dittmer*

Department of Microbiology and Immunology, The University of Oklahoma Health Sciences Center, Oklahoma City, Oklahoma 73104

Real-time quantitative PCR is used routinely for the high-throughput diagnosis of viral pathogens, such as West Nile virus (WNV). Rapidly evolving RNA viruses present a challenge for diagnosis because they accumulate mutations that may render them undetectable. To explore the effect of sequence variations on assay performance, we generated every possible single point mutation within the target region of the widely used TaqMan assay for WNV and found that the TaqMan assay failed to detect 47% of possible single nucleotide variations in the probe-binding site and was unable to detect any targets with more than two mutations. In response, we developed and validated a less expensive assay with the intercalating dye SYBR green. The SYBR green-based assay was as sensitive as the TaqMan assay for WNV. Importantly, it detected 100% of possible WNV target region variants. The assay developed here adds an additional layer of protection to guard against false-negative results that result from natural variations or drug-directed selection and provides a rapid means to identify such variants for subsequent detailed analysis.

West Nile virus (WNV) belongs to the *Flaviviridae*, a family of over 70 related viruses. Specifically, WNV is a member of the Japanese encephalitis (JE) serocomplex, which also includes JE virus, St. Louis encephalitis virus, Murray Valley encephalitis virus, and Kunjin virus (25). Like other flaviviruses, WNV is an enveloped, positive-sense RNA virus with a ca. 11-kb genome composed of three structural genes and seven nonstructural genes. The viral sequences for many isolates, such as WN-NY99 and others, have been determined (4–6, 9, 20, 23). WNV is arthropod borne and is maintained through an enzootic cycle between mosquitoes and birds. Humans and other mammals, such as horses, can be incidental dead-end hosts if bitten by an infected mosquito. In most cases, WNV causes a self-limited febrile illness; however, infection may also lead to encephalitis and death.

Originally isolated from the blood of a febrile Ugandan woman in 1937, WNV is widely distributed throughout Africa, the Middle East, areas of Europe, and Asia (31). The summer of 1999 marked the first incidence of WNV on the North American continent, in the northeastern United States (23). During this outbreak, more than 60 people became clinically ill, and seven deaths occurred due to encephalitis (12). WNV has continued to cause seasonal epidemics and to spread westward. In 2002, the virus was detected in 43 of 50 states, and more than 3,800 human cases were reported; 225 of these were fatal (8). Currently, no specific drug or vaccine against WNV is approved for human use, so that palliative care, nonspecific antiviral treatment (alpha interferon and ribavirin), surveillance, and screening of potentially contaminated products (such as blood) are the only available measures against WNV.

At the present time, enzyme-linked immunosorbent assays and PCR assays are used to monitor the presence of WNV (17, 22, 28). A real-time quantitative reverse transcriptase PCR (RT-QPCR) assay for WNV has been reported to enable routine high-throughput screening for WNV (19, 22). This assay is based on TaqMan technology; in addition to two specific outer primers, a third, fluorescence-labeled oligonucleotide (TaqMan) is used for detection. This assay has been proven to be as sensitive as gel-based reverse transcriptase PCR (RT-PCR), with a detection limit of 0.1 PFU/ml.

We have developed an alternative real-time RT-QPCR assay with the intercalating dye SYBR green. This assay is less expensive than TaqMan or beacon-based real-time quantitative PCR but is still faster than gel-based, single, or nested RT-PCR and should be economical for large-scale routine testing of clinical samples and blood products. Importantly, we found that this new assay is insensitive to nucleotide variations within the amplified region and thus has a substantially lower false-negative rate than prior assays. Furthermore, through dissociation curve analysis, the SYBR green-based RT-QPCR assay allows for the identification of novel WNV strains.

MATERIALS AND METHODS

Virus culture. Vero cells (American Type Culture Collection) were maintained in Dulbecco minimal essential medium supplemented with 10% fetal bovine serum and antibiotics (Cellgro Inc.) at 37°C in 5% CO_2. Confluent Vero cells (six-well plates) were incubated with 100 μl of a clarified suspension of WNV-positive tissue for 1 h. WNV-positive bird tissue (from 19 animals) was generously provided by the Oklahoma Animal Disease Diagnostic Laboratory. The clarified suspension was prepared by placing tissue samples into 5-ml snap-top tubes (Falcon 352063) together with 2 ml of homogenization buffer (2× phosphate-buffered saline, 0.05 M Tris-HCl [pH 7.6], 1% [wt/vol] bovine serum albumin, 4.2 mM sodium bicarbonate, 0.1 μg of streptomycin/ml, 1 μg of amphotericin B/ml) and four copper-clad steel beads (4.5 mm; Copperhand [Walmart Inc.]), and the mixture was vortexed for 45 s. The homogenate was subsequently centrifuged in 2-ml tubes (Sarstedt, Nümbrecht, Germany) at 13,000 rpm in an Eppendorf centrifuge for 5 min to remove solids from the supernatant. After incubation with 200 μl of a tissue-derived suspension, Vero

* Corresponding author. Mailing address: Department of Microbiology and Immunology, The University of Oklahoma Health Sciences Center, 940 Stanton L. Young Blvd., Oklahoma City, OK 73104. Phone: (405) 271-2133. Fax: (405) 271-3117. E-mail: dirk-dittmer@ouhsc.edu.
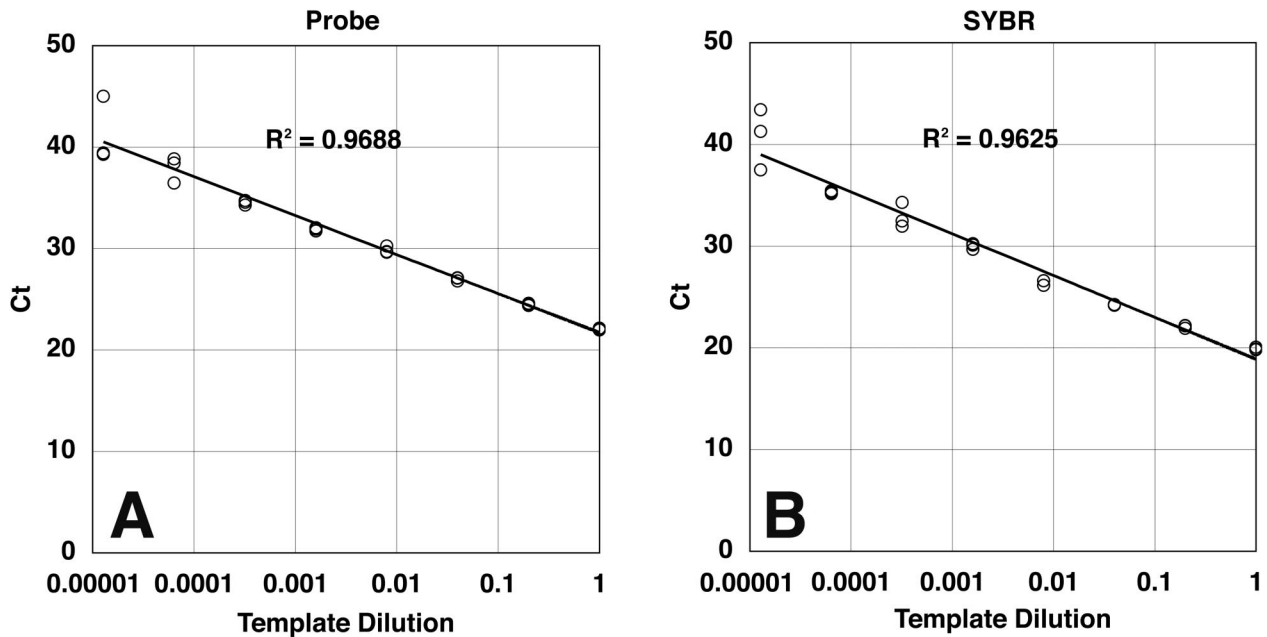
FIG. 1. Linearity and sensitivity comparisons of TaqMan and SYBR green-based real-time quantitative PCRs. Linear regression plots were generated for TaqMan and SYBR green-based real-time quantitative PCRs of WN-NY99 dilutions with the same WNV *env* primer set. The sample dilution on the horizontal axis is plotted against the C_T on the vertical axis ($n = 3$). (A) Linear regression of TaqMan assay. (B) Linear regression of SYBR green-based assay.

cell monolayers were observed daily for 7 days. For a plaque assay, 0.5% methylcellulose in 2× Dulbecco minimal essential medium was overlaid 2 h postabsorption. At the end of the observation period, the plates were fixed in 100% ice-cold methanol for 10 min, stained with 1% Giemsa stain (Sigma Inc., St. Louis, Mo.) for 30 min at room temperature, and rinsed with tap water.

RNA isolation and reverse transcription. RNA was isolated from the homogenate by using an Absolutely RNA Micro-Prep kit (Stratagene, La Jolla, Calif.) according to the manufacturer's instructions. Reverse transcription was performed as previously described (13). Briefly, 500 ng of RNA was reverse transcribed in a 20-μl reaction mixture with 100 U of SupercriptII reverse transcriptase (Invitrogen Inc., Carlsbad, Calif.), 2 mM deoxyribonucleoside triphosphates, 2.5 mM MgCl$_2$, 1 U of RNasin (the last three from Applied Biosystems, Foster City, Calif.), and 0.5 μg of random hexanucleotide primers (Amersham Pharmacia Biotech, Piscataway, N.J.). The reaction mixture was sequentially incubated at 42°C for 45 min, 52°C for 30 min, and 70°C for 10 min. The reverse transcription reaction was stopped by heating to 95°C for 5 min. Next, 0.5 U of RNase H (Invitrogen) was added, and the reaction mixture was incubated at 37°C for an additional 30 min. Afterward, the cDNA pool was diluted 25-fold with diethyl pyrocarbonate-treated, distilled H$_2$O and stored at −80°C.

Real-time quantitative PCR. The primers used for WNV in this study were previously described by Lanciotti et al. (22). They are 5′-TCA CGC ATC TCT CCA CCA AAG-3′ and 5′-GGG TCA GCA CGT TTG TCA TTG-3′ and are specific for the WNV *env* region. Positive control RNA (strain WN-NY99) was obtained from the Centers for Disease Control and Prevention Reference Laboratory (Ft. Collins, Colo.). Ninety-six variant 60-mer oligonucleotides were synthesized at The University of Oklahoma Health Sciences Center genomics facility. Real-time PCR was conducted with previously established procedures (11, 13). The final PCR mixture contained 2.5 μl each of forward and reverse primers (final concentration of each, 166 nM), 7.5 μl of 2× SYBR PCR mix (Applied Biosystems), and 5 μl of sample. The PCR was set up in a dedicated room with a CAS-1200 pipetting robot (Pheonix Research, Hayward, Calif.). The CAS-1200 robot uses filtered carbon-graphite pipette tips (Tecan Inc.) for liquid level sensing, allowing for a pipetting accuracy of 0.1 μl and eliminating carryover contamination. All surfaces were cleaned with 10% bleach and exposed to UV light overnight on a daily basis. Gowns, gloves, face masks, and equipment were required for all work. Real-time PCR was performed with an ABI Prism 5700 or ABI Prism 7700 machine (Applied Biosystems) and universal cycling conditions (2 min at 50°C, 10 min at 95°C, 40 cycles of 15 s at 95°C, and 1 min at 60°C). Cycle threshold (C_T) values were determined by automated threshold analysis with ABI Prism version 1.0 software. The amplification efficiencies were determined

by serial dilution and calculated as $E = \exp^{-1/m}$, where E is the amplification efficiency and m is the slope of the dilution curve. Dissociation curves were recorded after each run, and the amplified products were visualized by 2% agarose gel electrophoresis. The entire procedure from sample receipt to data analysis was routinely completed in 4 h.

Statistical analysis. Calculations were performed with Excel version 10.1 (Microsoft Inc., Redwood, Wash.) and SPSS version 12.0 (SPSS, Chicago, Ill.). Analysis of dissociation profiles was performed with ABI Prism version 1.0 software. The distance between dissociation profiles was calculated as a weighted sum of squares of differences between pairs of normalized data points. When necessary, linear interpolation was used between neighboring data points (10). Initially, dissociation profiles from 96 identical samples were compared to establish a detection threshold and overall measurement error. In later comparisons, all distances above the threshold were reported to be different from the reference.

RESULTS

SYBR green is as sensitive as TaqMan detection in a real-time RT-QPCR assay for WNV. A real-time RT-QPCR assay has been reported for the detection of WNV (22). We have adapted this assay by using primers designed on the basis of the envelope glycoprotein gene (WNV *env*) of strain WN-NY99. However, instead of using a specific fluorescence-labeled probe (TaqMan) for the detection of amplicons, we use SYBR green dye. Since SYBR green binds only to double-stranded and not to single stranded DNA molecules, PCR product concentrations can be recorded at each cycle, yielding a real-time amplification curve suitable for automated threshold analysis and quantification (24).

To compare the sensitivity of the SYBR green-based assay to that of the TaqMan assay, serial dilutions of strain WN-NY99 were tested in both assays with the WNV *env* probe and primer pairs previously described by Lanciotti et al. (22). Both assays performed with equal sensitivities and had similar linear

ranges (Fig. 1). C_T values for both assays were similar, with y-axis intercept points at the greatest dilution of 41.23 ± 3.26 (mean and standard error [SE]) and 40.72 ± 2.99 for TaqMan-based detection and SYBR green-based detection, respectively. The amplification efficiencies were identical, as evidenced by the identical slopes of the regression lines. The regression coefficients (R^2) for the TaqMan assay and the SYBR green-based assay were 0.9688 and 0.9625, respectively (Fig. 1). The parallel testing of these two detection methods establishes that the SYBR green-based assay is as sensitive as the TaqMan assay with the same (outer) PCR primers.

The sensitivity of SYBR green-based real-time RT-QPCR at low target concentrations ("real-world" conditions) was modeled by analyzing WNV in mosquito populations. Figure 2A shows the amplification plot for a representative set of mosquito pools (out of a total of 140). The two positive control reactions were practically superimposed upon each other (C_T, 22.06; associated SE, 0.41), attesting to the high reproducibility of our assay. Positive and negative samples segregated into two clearly distinguishable clusters, and the threshold was set accordingly. Conventional agarose gel electrophoresis confirmed the real-time RT-QPCR readings (Fig. 2B). WNV-positive samples could easily be distinguished from WNV-negative pools, which showed no amplification curve and no discernible band on the gel.

The specificity of SYBR green-based real-time RT-QPCR was ascertained by comparing the melting temperatures (T_ms) of the amplification products from different samples to that of the positive control sample (Fig. 2C). The T_m of the 60-bp WN-NY99 WNV *env* amplicon was 81.4°C. Cloning and sequencing of the PCR product yielded a sequence identical to the one previously deposited in GenBank under accession number AF196835 (data not shown). All samples that exhibited a T_m within ±1°C of that of the WN-NY99 control were considered positive for WNV. This threshold is based on extensive work with other viral assays (11, 13), which established the reproducibility of T_m profiles and their use for fingerprinting individual amplification products. Samples that yielded divergent T_m profiles are discussed below. SYBR green-based real-time quantitative PCR was as specific and as sensitive as TaqMan real-time quantitative PCR.

SYBR green-based real-time RT-QPCR can detect polymorphic targets, a property which lowers the overall false-negative rate. In screening natural WNV isolates, we encountered samples with a substantial viral load (as evidenced by low C_T values) but divergent dissociation profiles. These samples likely represented naturally occurring WNV variants with sequence variations within the amplicon and thus may have escaped detection by the TaqMan assay, yielding false-negative results. These samples yielded products which were indistinguishable from those yielded by the WN-NY99 sample (used as a positive control) in gel electrophoresis, since the readout in conventional or nested PCR is a band on a 2% agarose gel that can differentiate only gross variations in size (>5 bp, depending on the gel system) and not nucleotide substitutions. In contrast, the SYBR green-based assay provides an amplicon dissociation profile as an added measure of specificity. With this method, even single nucleotide changes can yield an altered profile, which should allow for the rapid routine detection of sequence variations.
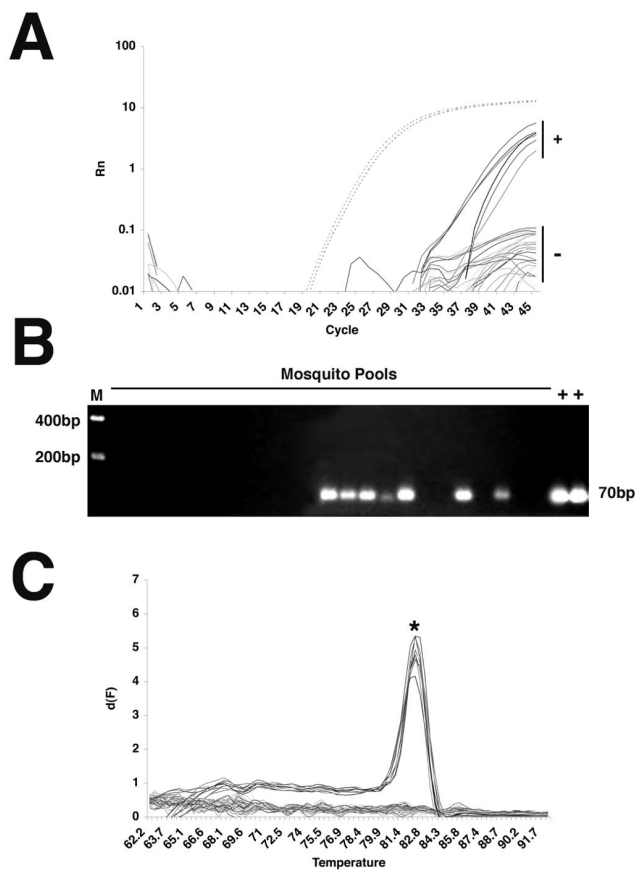

FIG. 2. Detection of WN virus in mosquito pools by SYBR green-based real-time RT-QPCR. (A) Plot of amplification of mosquito pools with the WNV *env* primer set. Cycle number on the horizontal axis is plotted against the relative fluorescence (Rn) on the vertical axis (log scale). Dotted lines indicate the two positive control reactions. Positive and negative mosquito pools are indicated by plus and minus signs, respectively. (B) Agarose (2%) gel electrophoresis of amplification products stained with ethidium bromide. Lane M, molecular weight markers. Lanes +, positive control (in duplicate). Positive reactions showed a single amplification product of approximately 60 bp. (C) Dissociation plot of amplification products for the positive control and mosquito pools. Temperature on the x axis is plotted against the first derivative of the measured fluorescence [d(F)] on the y axis. The asterisk indicates the peak position of the reference dissociation curve.

To compare directly the ability of the TaqMan assay and the SYBR green-based assay to detect polymorphisms, we synthesized 60-mer oligonucleotides containing every possible single point substitution in the central 28-bp amplicon region as well as selected double and triple mutations (Table 1). These oligonucleotides were each used as templates in both assays. As expected, all targets yielded a signal with SYBR green, but only 47 (53%) of 88 single-point-substitution amplicons were detected by the probe-based assay (Fig. 3A and B). This finding represents a false-negative rate of 47% for the TaqMan assay for single nucleotide polymorphisms across the probe-binding site. Of the eight double- and triple-substitution amplicons in our experiment, only five (63%) were detected by the TaqMan assay, even though a PCR product was amplified in all instances, as determined by agarose gel electrophoresis (Fig. 3C). This outcome indicates that WNV variants with multiple substitutions will escape detection by TaqMan real-time quan-

TABLE 1. Sequences of 60-mer mutant oligonucleotides that served as targets for amplification with WN *env* primers

Name	Sequence	Different melting profile[a]	Detected by TaqMan[b]
Wild type	TCAGCGATCTCTCCACCAAAGCTGCGTGCCCGACCATGGGAGAAGCTCA	0	1
1181C→A	TCAGCGATCTCTCCACCAAAGATGCGTGCCCGACCATGGGAGAAGCTCA	1	1
1181C→G	TCAGCGATCTCTCCACCAAAGGTGCGTGCCCGACCATGGGAGAAGCTCA	0	1
1181C→T	TCAGCGATCTCTCCACCAAAGTTGCGTGCCCGACCATGGGAGAAGCTCA	0	1
1182T→A	TCAGCGATCTCTCCACCAAAGCAGCGTGCCCGACCATGGGAGAAGCTCA	0	1
1182T→C	TCAGCGATCTCTCCACCAAAGCCGCGTGCCCGACCATGGGAGAAGCTCA	1	1
1182T→G	TCAGCGATCTCTCCACCAAAGCGGCGTGCCCGACCATGGGAGAAGCTCA	1	1
1183G→A	TCAGCGATCTCTCCACCAAAGCTACGTGCCCGACCATGGGAGAAGCTCA	1	1
1183G→C	TCAGCGATCTCTCCACCAAAGCTCCGTGCCCGACCATGGGAGAAGCTCA	0	0
1183G→T	TCAGCGATCTCTCCACCAAAGCTTCGTGCCCGACCATGGGAGAAGCTCA	1	0
1184C→A	TCAGCGATCTCTCCACCAAAGCTGAGTGCCCGACCATGGGAGAAGCTCA	1	0
1184C→G	TCAGCGATCTCTCCACCAAAGCTGGGTGCCCGACCATGGGAGAAGCTCA	0	0
1184C→T	TCAGCGATCTCTCCACCAAAGCTGTGTGCCCGACCATGGGAGAAGCTCA	0	0
1185G→A	TCAGCGATCTCTCCACCAAAGCTGCATGCCCGACCATGGGAGAAGCTCA	0	0
1185G→C	TCAGCGATCTCTCCACCAAAGCTGCCTGCCCGACCATGGGAGAAGCTCA	0	0
1185G→T	TCAGCGATCTCTCCACCAAAGCTGCTTGCCCGACCATGGGAGAAGCTCA	0	0
1186T→A	TCAGCGATCTCTCCACCAAAGCTGCGAGCCCGACCATGGGAGAAGCTCA	0	0
1186T→C	TCAGCGATCTCTCCACCAAAGCTGCGCGCCCGACCATGGGAGAAGCTCA	1	1
1186T→G	TCAGCGATCTCTCCACCAAAGCTGCGGGCCCGACCATGGGAGAAGCTCA	1	0
1187G→A	TCAGCGATCTCTCCACCAAAGCTGCGTACCCGACCATGGGAGAAGCTCA	1	0
1187G→C	TCAGCGATCTCTCCACCAAAGCTGCGTCCCCGACCATGGGAGAAGCTCA	0	0
1187G→T	TCAGCGATCTCTCCACCAAAGCTGCGTTCCCGACCATGGGAGAAGCTCA	0	0
1188C→A	TCAGCGATCTCTCCACCAAAGCTGCGTGACCGACCATGGGAGAAGCTCA	0	0
1188C→G	TCAGCGATCTCTCCACCAAAGCTGCGTGGCCGACCATGGGAGAAGCTCA	0	0
1188C→T	TCAGCGATCTCTCCACCAAAGCTGCGTGTCCGACCATGGGAGAAGCTCA	0	0
1189C→A	TCAGCGATCTCTCCACCAAAGCTGCGTGCACGACCATGGGAGAAGCTCA	0	0
1189C→G	TCAGCGATCTCTCCACCAAAGCTGCGTGCGCGACCATGGGAGAAGCTCA	0	0
1189C→T	TCAGCGATCTCTCCACCAAAGCTGCGTGCTCGACCATGGGAGAAGCTCA	0	0
1190C→A	TCAGCGATCTCTCCACCAAAGCTGCGTGCCAGACCATGGGAGAAGCTCA	0	0
1190C→G	TCAGCGATCTCTCCACCAAAGCTGCGTGCCGGACCATGGGAGAAGCTCA	0	0
1190C→T	TCAGCGATCTCTCCACCAAAGCTGCGTGCCTGACCATGGGAGAAGCTCA	0	0
1191G→A	TCAGCGATCTCTCCACCAAAGCTGCGTGCCCAACCATGGGAGAAGCTCA	0	0
1191G→C	TCAGCGATCTCTCCACCAAAGCTGCGTGCCCCACCATGGGAGAAGCTCA	0	0
1191G→T	TCAGCGATCTCTCCACCAAAGCTGCGTGCCCTACCATGGGAGAAGCTCA	0	0
1192A→C	TCAGCGATCTCTCCACCAAAGCTGCGTGCCCGCCCATGGGAGAAGCTCA	1	1
1192A→G	TCAGCGATCTCTCCACCAAAGCTGCGTGCCCGGCCATGGGAGAAGCTCA	0	0
1192A→T	TCAGCGATCTCTCCACCAAAGCTGCGTGCCCGTCCATGGGAGAAGCTCA	0	0
1193C→A	TCAGCGATCTCTCCACCAAAGCTGCGTGCCCGAACATGGGAGAAGCTCA	1	0
1193C→G	TCAGCGATCTCTCCACCAAAGCTGCGTGCCCGAGCATGGGAGAAGCTCA	0	0
1193C→T	TCAGCGATCTCTCCACCAAAGCTGCGTGCCCGATCATGGGAGAAGCTCA	0	0
1194C→A	TCAGCGATCTCTCCACCAAAGCTGCGTGCCCGACAATGGGAGAAGCTCA	0	0
1194C→G	TCAGCGATCTCTCCACCAAAGCTGCGTGCCCGACGATGGGAGAAGCTCA	0	0
1194C→T	TCAGCGATCTCTCCACCAAAGCTGCGTGCCCGACTATGGGAGAAGCTCA	0	0
1195A→C	TCAGCGATCTCTCCACCAAAGCTGCGTGCCCGACCCTGGGAGAAGCTCA	0	1
1195A→G	TCAGCGATCTCTCCACCAAAGCTGCGTGCCCGACCGTGGGAGAAGCTCA	1	0
1195A→T	TCAGCGATCTCTCCACCAAAGCTGCGTGCCCGACCTTGGGAGAAGCTCA	0	0
1196T→A	TCAGCGATCTCTCCACCAAAGCTGCGTGCCCGACCAAGGGAGAAGCTCA	0	0
1196T→C	TCAGCGATCTCTCCACCAAAGCTGCGTGCCCGACCACGGGAGAAGCTCA	0	1
1196T→G	TCAGCGATCTCTCCACCAAAGCTGCGTGCCCGACCAGGGGAGAAGCTCA	0	0
1197G→A	TCAGCGATCTCTCCACCAAAGCTGCGTGCCCGACCATAGGAGAAGCTCA	0	0
1197G→C	TCAGCGATCTCTCCACCAAAGCTGCGTGCCCGACCATCGGAGAAGCTCA	0	0
1197G→T	TCAGCGATCTCTCCACCAAAGCTGCGTGCCCGACCATTGGAGAAGCTCA	0	0
1198G→A	TCAGCGATCTCTCCACCAAAGCTGCGTGCCCGACCATGAGAGAAGCTCA	0	0
1198G→C	TCAGCGATCTCTCCACCAAAGCTGCGTGCCCGACCATGCGAGAAGCTCA	0	1
1198G→T	TCAGCGATCTCTCCACCAAAGCTGCGTGCCCGACCATGTGAGAAGCTCA	0	1
1199G→A	TCAGCGATCTCTCCACCAAAGCTGCGTGCCCGACCATGGAAGAAGCTCA	0	1
1199G→C	TCAGCGATCTCTCCACCAAAGCTGCGTGCCCGACCATGGCAGAAGCTCA	1	1
1199G→T	TCAGCGATCTCTCCACCAAAGCTGCGTGCCCGACCATGGTAGAAGCTCA	0	1
1200A→C	TCAGCGATCTCTCCACCAAAGCTGCGTGCCCGACCATGGGCGAAGCTCA	0	1
1200A→G	TCAGCGATCTCTCCACCAAAGCTGCGTGCCCGACCATGGGGGAAGCTCA	0	1
1200A→T	TCAGCGATCTCTCCACCAAAGCTGCGTGCCCGACCATGGGTGAAGCTCA	0	1
1201G→A	TCAGCGATCTCTCCACCAAAGCTGCGTGCCCGACCATGGGAAAAGCTCA	0	1
1201G→C	TCAGCGATCTCTCCACCAAAGCTGCGTGCCCGACCATGGGACAAGCTCA	0	1
1201G→T	TCAGCGATCTCTCCACCAAAGCTGCGTGCCCGACCATGGGATAAGCTCA	0	1
1202A→C	TCAGCGATCTCTCCACCAAAGCTGCGTGCCCGACCATGGGAGCAGCTCA	1	1
1202A→G	TCAGCGATCTCTCCACCAAAGCTGCGTGCCCGACCATGGGAGGAGCTCA	1	1
1202A→T	TCAGCGATCTCTCCACCAAAGCTGCGTGCCCGACCATGGGAGTAGCTCA	0	1
1203A→C	TCAGCGATCTCTCCACCAAAGCTGCGTGCCCGACCATGGGAGACGCTCA	1	1
1203A→G	TCAGCGATCTCTCCACCAAAGCTGCGTGCCCGACCATGGGAGAGGCTCA	0	1
1203A→T	TCAGCGATCTCTCCACCAAAGCTGCGTGCCCGACCATGGGAGATGCTCA	0	1

Continued on following page

TABLE 1—*Continued*

Name	Sequence	Different melting profile[a]	Detected by TaqMan[b]
1204G→A	TCAGCGATCTCTCCACCAAAGCTGCGTGCCCGACCATGGGAGAAACTCA	1	1
1204G→C	TCAGCGATCTCTCCACCAAAGCTGCGTGCCCGACCATGGGAGAACCTCA	0	1
1204G→T	TCAGCGATCTCTCCACCAAAGCTGCGTGCCCGACCATGGGAGAATCTCA	1	1
1205C→A	TCAGCGATCTCTCCACCAAAGCTGCGTGCCCGACCATGGGAGAAGATCA	1	1
1205C→G	TCAGCGATCTCTCCACCAAAGCTGCGTGCCCGACCATGGGAGAAGGTCA	0	1
1205C→T	TCAGCGATCTCTCCACCAAAGCTGCGTGCCCGACCATGGGAGAAGTTCA	0	1
1206T→A	TCAGCGATCTCTCCACCAAAGCTGCGTGCCCGACCATGGGAGAAGCACA	0	1
1206T→C	TCAGCGATCTCTCCACCAAAGCTGCGTGCCCGACCATGGGAGAAGCCCA	0	1
1206T→G	TCAGCGATCTCTCCACCAAAGCTGCGTGCCCGACCATGGGAGAAGCGCA	1	1
1207C→A	TCAGCGATCTCTCCACCAAAGCTGCGTGCCCGACCATGGGAGAAGCTAA	1	1
1207C→G	TCAGCGATCTCTCCACCAAAGCTGCGTGCCCGACCATGGGAGAAGCTGA	0	1
1207C→T	TCAGCGATCTCTCCACCAAAGCTGCGTGCCCGACCATGGGAGAAGCTTA	1	1
1208A→C	TCAGCGATCTCTCCACCAAAGCTGCGTGCCCGACCATGGGAGAAGCTCC	0	1
1208A→G	TCAGCGATCTCTCCACCAAAGCTGCGTGCCCGACCATGGGAGAAGCTCG	0	1
1208A→T	TCAGCGATCTCTCCACCAAAGCTGCGTGCCCGACCATGGGAGAAGCTCT	1	1
1181C→A, T→G	TCAGCGATCTCTCCACCAAAGAGGCGTGCCCGACCATGGGAGAAGCTCA	1	1
1181C→A, T→C	TCAGCGATCTCTCCACCAAAGACGCGTGCCCGACCATGGGAGAAGCTCA	1	1
1181C→T, T→G	TCAGCGATCTCTCCACCAAAGTGGCGTGCCCGACCATGGGAGAAGCTCA	0	1
1181C→T, T→C	TCAGCGATCTCTCCACCAAAGTCGCGTGCCCGACCATGGGAGAAGCTCA	0	1
1181C→A, 1183G→A, 1184C→T	TCAGCGATCTCTCCACCAAAGATATGTGCCCGACCATGGGAGAAGCTCA	1	0
1181C→A, 1189C→T, 1198G→A	TCAGCGATCTCTCCACCAAAGCTGCGTGCTCGACCATGAGAGAAGCTCA	1	0
1182T→G, 1186T→C, 1195A→G	TCAGCGATCTCTCCACCAAAGCGGCGCGCCCGGCCGTGGGAGAAGCTCA	1	0
1200A→C, 1203A→C, 1206T→G	TCAGCGATCTCTCCACCAAAGCTGCGTGCCCGACCATGGGCGGCGCTCA	1	1

[a] "1" denotes oligonucleotides which yielded a T_m and a dissociation curve that were significantly different from those of the wild type. "0" denotes oligonucleotides which yielded a T_m and dissociation curves that did not differ from those of the wild type.

[b] "0" denotes oligonucleotides which did not yield a detectable signal in the TaqMan assay. "1" denotes oligonucleotides which yielded a detectable signal.

titative PCR with a high probability, as would insertion or deletion mutants.

To explore the potential for the SYBR green-based assay to identify WNV mutants, all amplification products from the mutant oligonucleotide array were subjected to dissociation profile analysis (Fig. 3E). While every sequence with three or more substitutions could be easily recognized by the divergent dissociation profile, not all single or double nucleotide substitutions produced a dissociation profile that differed significantly from that of the wild-type sequence. Not surprisingly, among the single nucleotide substitutions that could be detected best were those with a strong (CG) to weak (AT) change or vice versa. The best result was obtained for T→G mutations (which are also transversions), 75% of which could be detected

by melting curve analysis. No T→A or C→G mutation could be detected, although we are currently optimizing the pattern recognition software (W. Vahrson and D. P. Dittmer, unpublished data). To assess the potential contributions of variations within the instrument to differences in T_ms, 96 reactions with WN-NY99 as the template were performed (Fig. 3D). Little to no variation (mean T_m, 83.9°C; SD, ±0.1°C; $n = 96$) was observed, indicating that differences in T_ms are due to differences in sequences and not to machine variations.

To determine how close the real-time PCR target area in WNV is to those in other flaviviruses or any other sequence, we performed a blastn (1) search of GenBank (Table 2). Within the first 100 hits based on sequence identity, 78 entries belonged to WNV sequences. Of these, 76 differed by no more

TABLE 2. Flavivirus sequences with significant similarity in the PCR target region[a]

Virus	GenBank identifier	Sequence	No. of identical entries in GenBank
WNV	38224786	TCAGCGATCTCTCCACCAAAGCTGCGTGCCCGACCATGGGAGAAGCTCACAATGACAAAC	43
	33242574	.............................A..............................	12
	16209495	..........T...	1
	16209491	....T....	8
	30983576	.................................G..........................	2
	4732136	....T.............	2
	6581069	....G.....C..........	1
	37147929	....T..................A....................................	7
	15919260	......T..A........T...........	1
	15919258	........T.....C...........G.	1
Kunjin	32306851	............G.........A.......G.....C..T.......G.	3
JE	1778267	..............C..G....	1
	32187331	.......C.....C..A....	7

[a] Multiple sequence alignment of the top 100 closest matches after a blastn search of GenBank (as of 9 December 2003). Shown are the GenBank identifier for each sequence class, the sequence alignment (identical residues are indicated by a dot), and the number of identical GenBank entries for individual viral isolates. No other members of the JE group or other members of the *Flaviviridae* family exhibit significant sequence homology in this region.
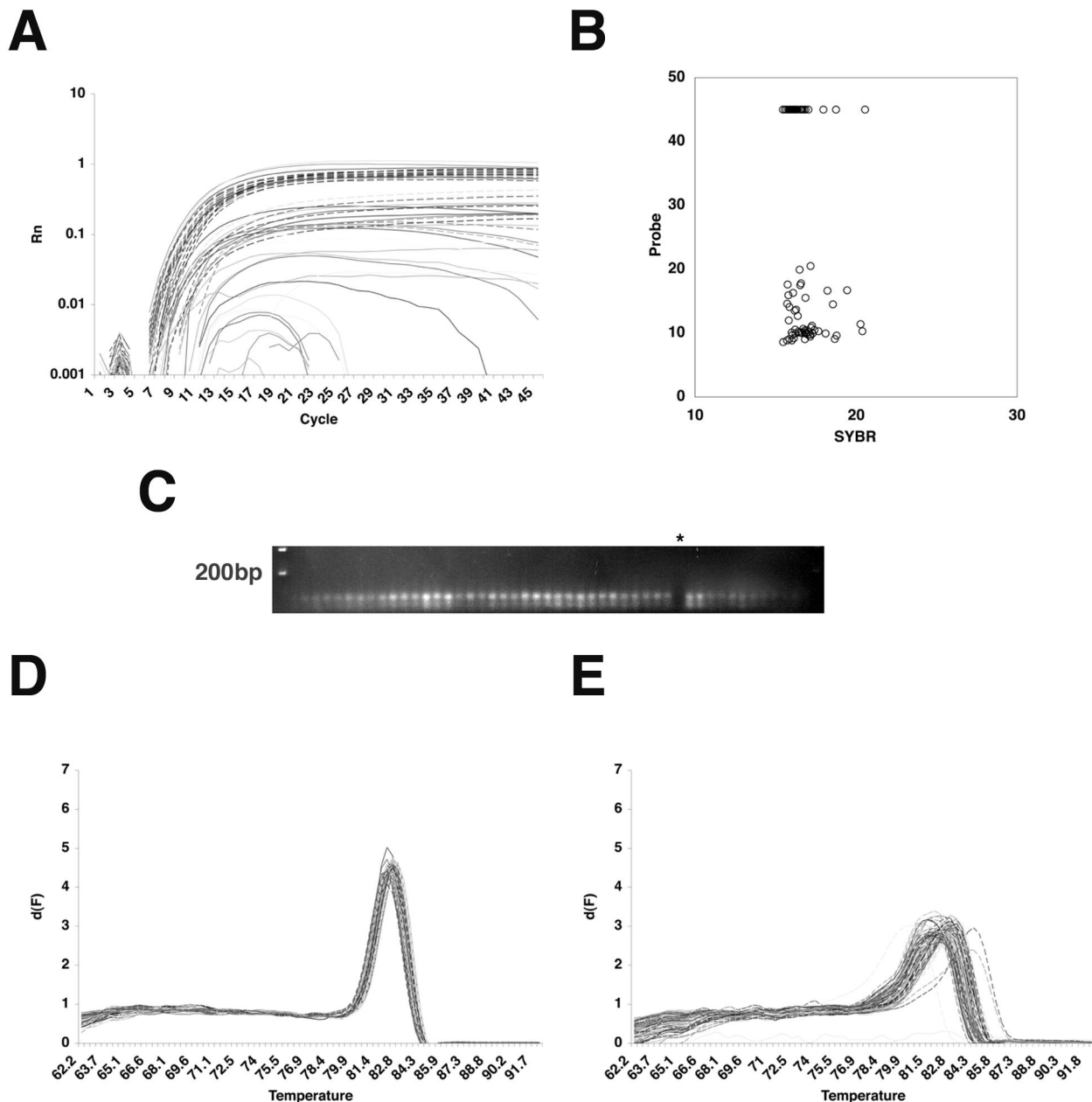
FIG. 3. Comparison of the effects of nucleotide variations on the TaqMan and SYBR green-based assays. (A) Plot of amplification of 96 mutant oligonucleotides in the SYBR green-based assay. The cycle number on the horizontal axis is plotted against the relative measured fluorescence (Rn) on the vertical axis. (B) C_T values obtained for individual mutant target oligonucleotides in either the SYBR green-based assay (horizontal axis) or the TaqMan assay (vertical axis). Samples that did not yield any signal were assigned a C_T value of 45. (C) Agarose (2%) gel electrophoresis of the amplification products from the TaqMan assay stained with ethidium bromide. The asterisk indicates an empty lane. (D) Dissociation plot of 96 identical samples (WN-NY99) after amplification in the SYBR green-based assay with the WNV *env* primer set. (E) Dissociation plot of the 96 mutant oligonucleotides listed in Table 1 after amplification in the SYBR green based assay with the WNV *env* primer set. The derivative of the measured fluorescence [d(F)] on the vertical axis is plotted against the temperature at which it was sampled on the horizontal axis for panels D and E.

than two nucleotides (96%) from the real-time quantitative PCR target sequence. The remaining two WNV sequences showed identity for 25 nucleotides (42%) and 27 nucleotides (45%). The next closest sequences were for three isolates classified as Kunjin virus, with 46 identical nucleotides (76%). JE virus isolates exhibited sequence identity in 20 nucleotide positions (33%) on the right side of this region only and thus would not have been recognized by the left-hand PCR primer.

All other flaviviruses exhibited no significant sequence similarity at the nucleotide level.

To determine whether the target copy number affected T_m-based typing, we performed limiting dilution analysis. WNV (strain OK02) was isolated in Vero cell cultures from the brain of a dead blue jay (data not shown). The supernatant from this culture was subjected to fivefold serial dilution, and RNA was subsequently purified. Even after multiple dilution steps, sam-

ples that were amplified above the background had the same T_m profile as the positive control sample (Fig. 4). This finding demonstrated that the T_m and dissociation profiles are independent of the initial target concentration.

To improve our dissociation profile analysis, we applied a mathematical algorithm that takes into account the shape of the entire dissociation profile rather than the single data point for T_m (implementation of a standard graph comparison as described previously [10]; Vahrson and Dittmer, unpublished). This algorithm recognized 23 (27%) of all 84 single point mutations in the target sequence, even though the difference in T_m from the original target sequence was only 1.5°C ± 0.5°C. These mutations would not have been detected by inspection of the T_m alone. Interestingly, the algorithm performed much better with particular types of substitutions; e.g., 75% of all T→G substitutions were detected, while no T→A substitutions could be detected. It recognized 50% of double nucleotide substitutions in the target sequence and 100% of all triple nucleotide substitutions. It is clear that dissociation profile analysis does not substitute for single-nucleotide-polymorphism analysis for the detection of specific mutants or defined genotypes (14, 16, 18, 30). However, in the context of routine screening, samples with an aberrant dissociation profile indicate variant WNV strains, which then may be selected for detailed characterization by sequence analysis.

DISCUSSION

We developed and validated an improved real-time RT-QPCR assay for WNV. Detection with SYBR green is as sensitive as probe-based real-time PCR without the need for a specialized probe (Fig. 1). All samples that yielded a fluorescence signal at least five times that of the nontemplate control reaction in the SYBR green-based assay also produced an easily discernible band upon agarose gel electrophoresis. Hence, these samples would be considered positive by conventional end-point RT-PCR. Using a pipetting robot, we were able to detect WNV in field samples with a 15-μl RT-PCR. Using previously published WNV *env* primers, we achieved an SE for C_T values of less than 1% in a 96-sample repeat experiment (Fig. 3 and data not shown). Lanciotti and colleagues introduced the TaqMan primers and probe for WNV used here and also, more recently, nucleic acid sequence-based amplification (NASBA) for WNV (21, 22). Their comparison of TaqMan real-time RT-QPCR, NASBA, and conventional RT-PCR revealed a strong concordance for all three methods, except for operator-based interpretations of threshold settings for NASBA and real-time RT-QPCR at very low target levels (≤0.1 PFU/ml). We found that real-time quantitative PCR with SYBR green also has a comparable performance profile. Comparisons at the extreme lower end of the linear range between different amplification methods are difficult to interpret, since different primer pairs with associated different amplification efficiencies (27) and different reagents (13) have been used. Previous studies estimated the limit of detection for the probe-based TaqMan RT-QPCR assay for WNV to be ≤0.1 PFU/ml (2, 22, 26, 28), well below the detection limit for culture-based assays. Using serial dilutions on Vero cells (Fig. 4), we confirmed these observations for SYBR green-based real-time quantitative PCR.

The possibility of false-negative test results poses a substantial problem in diagnostic TaqMan assays because mutations within the probe-binding site can prevent annealing of the probe and subsequent detection. While this problem has been documented for herpes simplex virus (3), it is a particular concern for WNV, severe acute respiratory syndrome virus, human immunodeficiency virus, hepatitis C virus, and other RNA viruses, since they exhibit higher sequence variability than DNA viruses and since it is not always possible to identify regions of the genome which are highly conserved. By synthesizing and testing every possible point mutation in the target region for the widely used WNV TaqMan assay, we encountered a potential false-negative rate of 47% for the TaqMan assay due to sequence variations in the probe-binding site. In comparison, the SYBR green-based assay produced a false-positive rate of 0% (Fig. 3). We did not explore the effects of mutations within the binding sites for the forward and reverse primers, since these would affect the TaqMan assay and the SYBR green-based assay (as well as gel-based PCR assays) in the same way. The high-stringency annealing temperature used in real-time quantitative PCR (60°C) for the two outer primers leaves open the possibility that viral variants with mutations in the forward or reverse primer-binding sites may escape detection. Although not tested here, it is likely that the frequency of
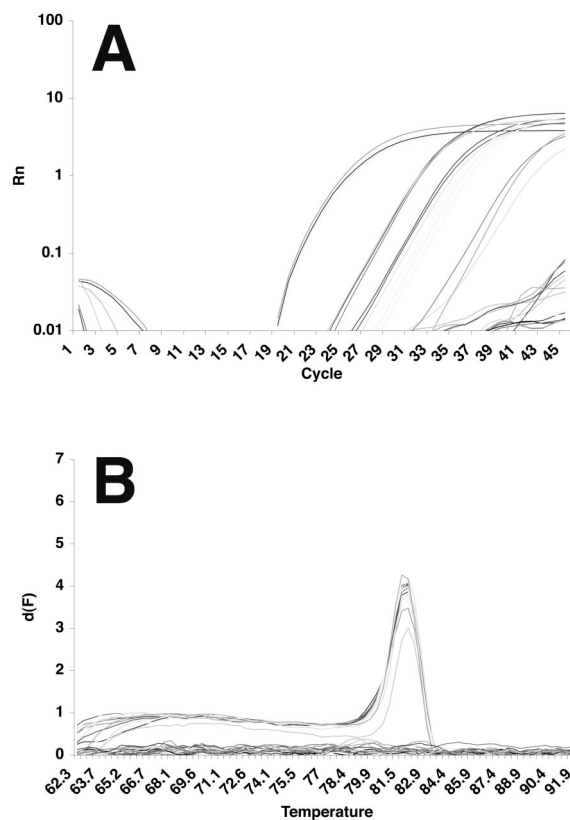

FIG. 4. Titration of WNV from an avian sample in a Vero cell culture. (A) Plot of amplification of serially diluted supernatants from infected Vero cell cultures. The cycle number on the horizontal axis is plotted against the relative measured fluorescence (Rn) on the vertical axis. (B) Dissociation plot of amplification products. The temperature on the horizontal axis is plotted against the derivative of the measured fluorescence [d(F)] on the vertical axis.

such false-negatives can be reduced by the use of multiple primer sets for each virus.

Could a SYBR green-based real-time PCR assay be used to screen for novel WNV isolates? A number of studies investigated WNV sequence variability (2, 4, 20, 23, 29). For this flavivirus, the average sequence variability did not exceed 3% at the nucleotide level, and the majority of mutations did not lead to amino acid substitutions. For the 1999 outbreak in New York, Connecticut, and New Jersey, 99% sequence identity was reported over a 1,278-nucleotide region in 13 isolates from avian species, humans, and mosquitoes. Many of the same mutations were shared among isolates from mosquitoes, birds, and humans. Presumably, the need to enter and replicate in cells of avian as well as arthropod origins places severe constraints on the variability of this virus. In contrast, human retroviruses, such as human immunodeficiency virus type 1 (15), exhibit amino acid variability of up to 20% within the same subtype. We found that a preliminary measure of natural variability can be obtained by T_m or dissociation profile analysis (Fig. 3). SYBR green-based real-time quantitative PCR incorporates dissociation profile analysis for each sample at no extra cost. This feature constitutes a considerable improvement over gel-based or TaqMan-based PCR, neither of which can identify the presence of single nucleotide mutations or small (<5-bp) insertions or deletions. In the TaqMan assay, these alterations led to a complete loss of signal (false-negative) or produced signals that were indiscernible from the wild-type signal (Fig. 3); in the gel-based assay, the signals produced by these mutations were indiscernible from the wild-type signal. Since real-time quantitative PCR amplicons are small (<100 bp), even a single base-pair change can result in a distinguishable change in the T_m (7), although in this study only changes of >3 nucleotides were identified with 100% accuracy. Currently, we are trying to improve upon the bioinformatics tools for this analysis. While not as reliable as sequence analysis, dissociation profile analysis has the potential to be used for rapid initial screening for the identification of viral mutants.

ACKNOWLEDGMENTS

REFERENCES

1. **Altschul, S. F., T. L. Madden, A. A. Schaffer, J. Zhang, Z. Zhang, W. Miller, and D. J. Lipman.** 1997. Gapped BLAST and PSI-BLAST: a new generation of protein database search programs. Nucleic Acids Res. **25:**3389–3402.
2. **Anderson, J. F., T. G. Andreadis, C. R. Vossbrinck, S. Tirrel, E. Wakem, R. French, A. Garmendia, and H. Van Kruiningen.** 1999. Isolation of West Nile virus from mosquitoes, crows, and a Cooper's hawk in Connecticut. Science **286:**2331–2333.
3. **Anderson, T. P., A. M. Werno, K. A. Beynon, and D. R. Murdoch.** 2003. Failure to genotype herpes simplex virus by real-time PCR assay and melting curve analysis due to sequence variation within probe binding sites. J. Clin. Microbiol. **41:**2135–2137.
4. **Beasley, D. W., C. T. Davis, H. Guzman, D. L. Vanlandingham, A. P. Travassos da Rosa, R. E. Parsons, S. Higgs, R. B. Tesh, and A. D. Barrett.** 2003. Limited evolution of West Nile virus has occurred during its southwesterly spread in the United States. Virology **309:**190–195.
5. **Beasley, D. W., L. Li, M. T. Suderman, and A. D. Barrett.** 2002. Mouse neuroinvasive phenotype of West Nile virus strains varies depending upon virus genotype. Virology **296:**17–23.
6. **Brinton, M. A.** 2002. The molecular biology of West Nile virus: a new invader of the western hemisphere. Annu. Rev. Microbiol. **56:**371–402.
7. **Cantor, C. R., and P. R. Schimmel.** 1980. Biophysical chemistry: the behavior of biological macromolecules. W. H. Freeman & Co., New York, N.Y.
8. **Centers for Disease Control and Prevention.** 2002. West Nile virus activity—United States, July 31-August 7, 2002, and Louisiana, January 1-August 7, 2002. Morb. Mortal. Wkly. Rep. **51:**681–683.
9. **Chambers, T., M. Halevy, A. Nestorowicz, C. Rice, and S. Lustig.** 1998. West Nile virus envelope proteins: nucleotide sequence analysis of strains differing in mouse neuroinvasiveness. J. Gen. Virol. **79:**2375–2380.
10. **Chatfield, C., and A. J. Collins.** 1980. Introduction to multivariate analysis. Chapman & Hall, Ltd., London, England.
11. **Dittmer, D. P.** 2003. Transcription profile of Kaposi's sarcoma-associated herpesvirus in primary Kaposi's sarcoma lesions as determined by real-time PCR arrays. Cancer Res. **63:**2010–2015.
12. **Enserink, M.** 2002. West Nile's surprisingly swift continental sweep. Science **297:**1988–1989.
13. **Fakhari, F. D., and D. P. Dittmer.** 2002. Charting latency transcripts in Kaposi's sarcoma-associated herpesvirus by whole-genome real-time quantitative PCR. J. Virol. **76:**6213–6223.
14. **Gardner, S. N., T. A. Kuczmarski, E. A. Vitalis, and T. R. Slezak.** 2003. Limitations of TaqMan PCR for detecting divergent viral pathogens illustrated by hepatitis A, B, C, and E viruses and human immunodeficiency virus. J. Clin. Microbiol. **41:**2417–2427.
15. **Gaschen, B., J. Taylor, K. Yusim, B. Foley, F. Gao, D. Lang, V. Novitsky, B. Haynes, B. H. Hahn, T. Bhattacharya, and B. Korber.** 2002. Diversity considerations in HIV-1 vaccine selection. Science **296:**2354–2360.
16. **Harris, E., E. Sandoval, A. M. Xet-Mull, M. Johnson, and L. W. Riley.** 1999. Rapid subtyping of dengue viruses by restriction site-specific (RSS)-PCR. Virology **253:**86–95.
17. **Hunt, A. R., R. A. Hall, A. J. Kerst, R. S. Nasci, H. M. Savage, N. A. Panella, K. Gottfried, K. L. Burkhalter, and J. T. Roehrig.** 2002. Detection of West Nile virus antigen in mosquitoes and avian tissues by a monoclonal antibody-based capture enzyme immunoassay. J. Clin. Microbiol. **4:**2023–2030.
18. **Ito, Y., J. C. Grivel, and L. Margolis.** 2003. Real-time PCR assay of individual human immunodeficiency virus type 1 variants in coinfected human lymphoid tissues. J. Clin. Microbiol. **41:**2126–2131.
19. **Kauffman, E. B., S. A. Jones, A. P. Dupuis II, K. A. Ngo, K. A. Bernard, and L. D. Kramer.** 2003. Virus detection protocols for West Nile virus in vertebrate and mosquito specimens. J. Clin. Microbiol. **41:**3661–3667.
20. **Lanciotti, R. S., G. D. Ebel, V. Deubel, A. J. Kerst, S. Murri, R. Meyer, M. Bowen, N. McKinney, W. E. Morrill, M. B. Crabtree, L. D. Kramer, and J. T. Roehrig.** 2002. Complete genome sequences and phylogenetic analysis of West Nile virus strains isolated from the United States, Europe, and the Middle East. Virology **298:**96–105.
21. **Lanciotti, R. S., and A. J. Kerst.** 2001. Nucleic acid sequence-based amplification assays for rapid detection of West Nile and St. Louis encephalitis viruses. J. Clin. Microbiol. **39:**4506–4513.
22. **Lanciotti, R. S., A. J. Kerst, R. S. Nasci, M. S. Godsey, C. J. Mitchell, H. M. Savage, N. Komar, N. A. Panella, B. C. Allen, K. E. Volpe, B. S. Davis, and J. T. Roehrig.** 2000. Rapid detection of West Nile virus from human clinical specimens, field-collected mosquitoes, and avian samples by a TaqMan reverse transcriptase PCR assay. J. Clin. Microbiol. **38:**4066–4071.
23. **Lanciotti, R. S., J. T. Roehrig, V. Deubel, J. Smith, M. Parker, K. Steele, et al.** 1999. Origin of the West Nile virus responsible for an outbreak of encephalitis in the northeastern United States. Science **286:**2333–2337.
24. **Morrison, T. B., J. J. Weis, and C. T. Wittwer.** 1998. Quantification of low-copy transcripts by continuous SYBR Green I monitoring during amplification. BioTechniques **24:**954–958, 960, 962.
25. **Murphy, F., C. Fauquet, D. Bishop, S. Ghabrail, A. Jarvis, G. Martelli, M. Mayo, and M. Summers.** 1995. Virus taxonomy, classification and nomenclature of viruses. Arch. Virol. **10:**1–58.
26. **Nasci, R. S., D. J. White, H. J. Stirling, J. Oliver, T. J. Daniels, R. C. Falco, S. Campbell, W. J. Crans, H. M. Savage, R. S. Lanciotti, C. G. Moore, M. S. Godsey, K. Gottfried, and C. J. Mitchell.** 2001. West Nile virus isolates from mosquitoes in New York and New Jersey, 1999. Emerg. Infect. Dis. **7:**626–630.
27. **Pfaffl, M. W.** 2001. A new mathematical model for relative quantification in real-time RT-PCR. Nucleic Acids Res. **29:**e45.
28. **Shi, P.-Y.** 2001. High-throughput detection of West Nile virus RNA. J. Clin. Microbiol. **39:**1264–1271.
29. **Shi, P.-Y., M. Tilgner, M. K. Lo, K. A. Kent, and K. Bernard.** 2002. Infectious cDNA clone of the epidemic West Nile virus from New York City. J. Virol. **76:**5847–5856.
30. **Shu, P. Y., S. F. Chang, Y. C. Kuo, Y. Y. Yueh, L. J. Chien, C. L. Sue, T. H. Lin, and J. H. Huang.** 2003. Development of group- and serotype-specific one-step SYBR green I-based real-time reverse transcription-PCR assay for dengue virus. J. Clin. Microbiol. **41:**2408–2416.
31. **Smithburn, K., T. Hughes, A. Burke, and J. Paul.** 1940. A neurotropic virus isolated from the blood of a native of Uganda. Am. J. Trop. Med. Hyg. **20:**471–492.